7. A Study of Slabstock Flexible Polyurethane Foams Based on Varied Toluene Diisocyanate Isomer Ratios

7.1 Chapter Summary

The morphological features of three flexible slabstock polyurethane foams based on varied contents of the 2,4 and 2,6 toluene diisocyanate (TDI) isomers have been investigated. The three commercially available TDI mixtures, i.e., 65:35 2,4/2,6 TDI, 80:20 2,4/2,6 TDI, and 100:0 2,4/2,6 TDI were utilized. The foams were characterized at different length scales using several techniques. Differences in the cellular structure of the foams were noted using SEM. SAXS was used to demonstrate that all the three foams were microphase separated and possessed similar interdomain spacings. TEM revealed that the aggregation of the urea phase into large urea rich regions decreased systematically on increasing the asymmetric TDI isomer content. FTIR showed that the level of bidentate hydrogen bonding of the hard segments increased with the 2,6 TDI isomer content. DSC and DMA were used to note changes in the soft segment glass transition temperature of the foams on varying the diisocyanate ratios and suggested that the perfection of microphase separation was enhanced on increasing the 2,6 TDI isomer content. The above observations were utilized to explain why the foam containing the highest content of the symmetric 2,6 TDI isomer exhibited the highest rubbery storage modulus, as measured by DMA.

7.2 Introduction

Polyurethanes are a broad class of materials which find applications in the areas of foams, fibers, elastomers, coatings, and adhesives.[1] The mechanical properties of polyurethanes are strongly influenced by the microphase separated morphology which results from an incompatibility between soft flexible aliphatic polyether (or polyester) segments alternating with the commonly utilized aromatic, isocyanate-based hard segments. The hard segments which are formed from the reaction of an isocyanate moiety with a chain extender containing amine or alcohol groups, react with the soft segments forming urethane linkages. SAXS has been widely used to investigate the microphase separated morphology of polyurethanes, for example in the studies by Neumüller et. al.,[2] Tyagi et. al.,[3] and Koberstein et. al.[4] This phase separated morphology is known to play a key role in determining the overall polymer properties and has been of interest to several workers.[5, 6] More recently, the use of AFM to probe phase separation

in polyurethane[7] and poly(urethane urea)[8] elastomers, as well as in polyurethane foams[9, 10] has also been reported.

An important application of polyurethanes is the area of flexible polyurethane foams which are used in transportation, packaging, and furnishing applications.[11] This class of polyurethanes typically contains water-extended, toluene diisocyanate based urea hard segments which are covalently bound to soft polyether segments based on ethylene oxide, or propylene oxide, or both kinds of repeating units. When the concentration of the urea segments exceeds a system dependent solubility limit, they microphase separate and form urea microdomains. Also, the reaction of water with the isocyanate component is known to result in the production of carbon dioxide, which along with the heat generated due to the exothermic nature of the reactions, helps in expanding the foaming reactants and giving the foam its cellular structure. In addition to the microphase separation discussed above, another level of structure is known to exist in the solid portion of flexible polyurethane foams. Workers have observed using TEM and x-ray microscopy (XRM), the presence of urea rich macrophases, ca. 0.3 μm in size, which are commonly referred to as urea 'balls' or urea 'aggregates'.[11, 12] These macrophases have been noted to be more pronounced in slabstock formulations as compared to molded formulations with similar hard segment contents.[11]

Flexible polyurethane foam production in North America relies heavily on the commercially available 80:20 2,4/2,6 TDI mixture, although some European countries also utilize MDI. Structure-property relationships of foams based on the 80:20 2,4/2,6 TDI mixture have been studied extensively and are available in the literature.[11, 13, 14, 15] There are also commercially available the pure 2,4 TDI isomer and the 65:35 2,4/2,6 TDI mixture - however, the literature describing foams based on these isocyanates is relatively sparse.[16, 17] Also, the pure 2,6 TDI isomer is far more expensive than the pure 2,4 TDI isomer and the other two commercial mixtures, and has therefore found no economically feasible applications.

The 2,4 vs 2,6 TDI isomers differ markedly with respect to their structure as well as reactivity. The chemical structures of the two isomers are shown in Figure 7.1. Firstly, the 2,6 isomer is symmetric as compared to the 2,4 isomer, and is therefore expected to form hard segments which have better packing characteristics. Secondly, the relative reaction rates of the different isocyanate groups on each molecule differ significantly.[11] The reactivity of the *ortho* position in the 2,4 isomer is known to be approximately 12% of the reactivity of the isocyanate

group in the *para* position due to the steric hindrance caused by the methyl group. However, when the reaction temperature approaches 100 °C, steric hindrance effects are overcome and both the positions react at nearly the same rate. In comparison, the isocyanate groups on the 2,6 isomer have equal reactivities when both groups are unreacted. However, after one of the isocyanate groups reacts, the reactivity of the second group drops by a factor of ca. 3.

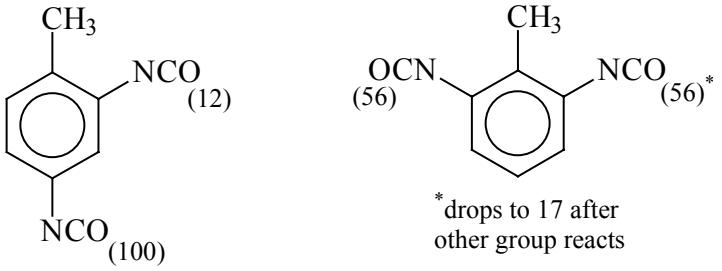

2,4 TDI 2,6 TDI

Figure 7.1 The chemical structures of 2,4 and 2,6 TDI isomers. The numbers indicate relative rates of reaction of the isocyanate groups at the different positions.

As mentioned earlier, there are only very limited studies which describe the effect of varying the ratio of the 2,4 vs. 2,6 isomers on the structure-property relationships of flexible polyurethane foams.[16, 17] However, the influence of this variable has been somewhat more extensively studied in the area of polyurethane elastomers. For instance, Sung and Schneider carried out infrared studies on polyurethane elastomers based on the pure 2,4 and 2,6 TDI isomers which utilized poly(tetramethylene oxide) (PTMO) as the soft segment and 1,4-butanediol (BDO) as the chain extender.[18] They reported that in the 2,6 TDI polyurethanes, 80% of the carbonyl groups were hydrogen bonded to urethane NH groups, where as in comparable 2,4 systems, only 50% of the carbonyl groups were hydrogen bonded. Nierzwicki also studied PTMO/BDO based polyurethane elastomers which utilized varied contents of the 2,4 and 2,6 TDI isomers.[19] In that study, it was observed that increasing the content of the 2,6 TDI isomer led to a systematic increase in both the tensile strength as well as the modulus of the elastomers investigated. It was suggested that the symmetric nature of the 2,6 TDI isomer enhanced the "stiffness" of the hard domains. Also, in the same study, the soft segment glass transition temperature was found to decrease as the 2,6 TDI isomer content was increased, which suggested that the perfection of the microphase separation was enhanced on increasing the content of the symmetric 2,6 TDI isomer.

Molau has described the influence of varying the content of 'A' and 'B' blocks on the morphology of an 'A-B' block copolymer.[20] On increasing the volume fraction (ϕ) of component A in a mixture of A and B phases, the morphology was described as spheres of A in a matrix of B (for $\phi_A < 20\%$), cylinders of A in a matrix of B (for $20\% \leq \phi_A \leq 35\%$), and as an alternating lamellar structure for $35\% \leq \phi_A \leq 50\%$. Phase inversion occurs on further increasing the content of component A which then leads to component B being dispersed in a similar manner in a matrix of component A. In addition to these morphologies, the presence of a gyroid phase has also been predicted[21] and recently discussed by Bates and Fredrickson.[22] These idealized morphologies reflect that the on increasing the content of, say component A in B, a more continuous and connected texture of A is established. Although polyurethane foams, and other segmented polyurethanes in general, do not exhibit these systematic morphologies due to their segmented nature, and polydispersity of the segments; it is expected based on volume fraction arguments, that on exceeding a certain hard segment content, the connectivity of the urea hard phase would occur which in turn would strongly affect mechanical and related properties. In fact, on studying segmented polyurethane elastomers with varied hard segment content, the formation of an interlocking connected morphology at a hard segment content of ca. 35 wt % was proposed by Abouzahr and Wilkes.[5] Also, in a study carried out on a series of polyurethane elastomers of different hard segment content, Seymour and Cooper concluded that above a certain hard segment content, ca. 25%, it is impossible, due to spatial limitations, to have discrete separated microdomains.[23] They also suggested that instead, an interlocking microdomain morphology developed. The connectivity of the urea hard phase is thus thought to play an important role in determining structure-property relationships of the current class of foams investigated which have a hard segment content of ca. 32 wt %.

As discussed in a recent study from our laboratory, urea phase connectivity in polyurethane foams is thought to be present at different scale lengths.[10] Hydrogen bonding between adjacent urea hard segments leads to connectivity of the urea phase at the segmental level. There is also the possibility of the larger scale urea aggregates in polyurethane foams to have physical associations with each other and thus provide connectivity at the urea aggregate level. These issues will be raised later to explain the dynamic mechanical behavior of the foams discussed in the present study.

7.3 Experimental

7.3.1 Materials

The three commercially available mixtures of the TDI isomers, namely 65:35 2,4/2,6 TDI; 80:20 2,4/2,6 TDI; and 100:0 2,4/2,6 TDI were used to synthesize foams to investigate the effect of varying the isomer ratios. These foams were supplied by Dow Chemical. The foams utilized Voranol 3322® which has an equivalent weight of 1220 with an EO content of 12.5 %. Water level was maintained at 5 pphp and an isocyanate index of 105 was used which led to all foams containing approximately 32% hard segment content by weight. The foams also made use of 1.2 pphp BF2370 (surfactant), and catalyst contents were 0.09 pphp Dabco 33LV, and 0.02pphp Niax A1. Dabco 33LV is 33 % triethylene diamine in propylene glycol; Niax A1 is a 70:30 mixture of bis(dimethylaminoethyl) ether and dipropylene glycol. In order to obtain foams

Sample →	**T65**	**T80**	**T100**
Voranol 3322	100	100	100
Water (pphp)	5.0	5.0	5.0
TDI index	105	105	105
Dabco 33LV (pphp)	0.09	0.09	0.09
Niax A1 (pphp)	0.02	0.02	0.02
Dabco T9 (pphp)	0.3	0.2	0.1
Foam density (kg/m^3)	22.6	22.2	23.2

Table 7.1 Formulations utilized for foam preparation

with nearly constant bulk densities, the content of Dabco T9, which is a stabilized stannous octoate catalyst, was varied for the three foams as shown in Table 7.1. The bulk densities of the foams are also mentioned in the same table. The nomenclature used for referring to the foams is straightforward. The foams which contain the 65:35 2,4/2,6 TDI isomer, 80:20 2,4/2,6 TDI isomer, and 100:0 2,4/2,6 TDI isomer are labeled as T65, T80, and T100 respectively.

7.3.2 Methods

Characterization of the cellular-structure of the foams was performed using a Leo 1550 field-emission scanning electron microscope (FE-SEM). This technique gives information about the cell sizes, cell size distribution, and strut thickness of the foam. In addition, it also reveals the

anisotropy in the cellular structure of *slabstock* polyurethane foams which blow under free conditions and result in cells which are elongated along the blow or rise direction.[11, 13] Foam samples of ca. 5 mm thickness were mounted to aluminum stubs using copper tape. The samples were then coated with a ca. 15 nm gold layer using a sputter coater. The microscope was operated at 5 kV and images were taken at a magnification of 30x.

To investigate the local ordering of the hard segments at the 1-10 Å level, wide angle x-ray scattering (WAXS) was employed. WAXS experiments were carried out using a Phillips model PW1720 generator equipped with a Warhus camera. Pinhole collimated (ca. 0.02 in. diameter), nickel filtered CuKα radiation with a wavelength of 1.542 Å was used. Foam samples were cut approximately 15 mm thick and compressed to ca. 3 mm before exposure to x-rays. The sample to film distance for the foam samples was 5.5 cm and exposure times were ca. 8 hours. The compression of foams in order to carry out x-ray scattering experiments is common practice as has been reported in previous studies.[9, 13] The degree of compression is only to densify the initial foam so as to reduce the sample thickness which helps minimize line broadening effects in the WAXS experiment. The compression load is not so great so as to alter the morphological features of the microphase texture since complete reversibility (expansion) occurs upon release of the compressive load.

Small angle X-ray scattering (SAXS) was utilized to study the microphase separation characteristics of the foams investigated. The x-ray source was a Philips model PW1729 generator operating at 40 kV and 20 mA. A Kratky camera with slit collimated (0.03 x 5 mm^2) nickel filtered CuKα radiation having a wavelength of 1.542 Å was utilized. The detector used was a Braun OED 50 position-sensitive platinum wire detector. The raw data was corrected for parasitic scattering and normalized using a Lupolen standard. Foam samples were cut approximately 10 mm thick and then compressed to approximately 3 mm, before exposing to x-rays.

Fourier transform infrared (FTIR) spectroscopy was utilized to evaluate the hydrogen bonding characteristics of the materials studied. A Nicolet 510 spectrometer with a Spectra-Tech ATR attachment utilizing a horizontal ZnSe crystal was used. The collected spectra were analyzed using Omnic 3.0 software. The scans were normalized using the CH_2 absorbance which occurs at 2970 cm^{-1}.

Transmission electron microscopy (TEM) was used to examine the effect of varying the isomer ratios on the urea aggregation behavior. Small samples were cut from the center of the foam buns and embedded in epoxy which was allowed to cure overnight at ambient conditions. No changes in the sample dimensions were noted before and after the embedding, suggesting that there was no chemical interaction between the epoxy and the samples. The samples were then trimmed using a razor blade in order to expose a single foam strut to the surface. A diamond knife was used to cryogenically microtome the trimmed surfaces into ultra-thin sections (ca. 80 nm) on a Reichert-Jung ultramicrotome Ultracut E equipped with a model FC-4D cryo-attachment operating at –90°C. The microtomed sections were collected on 600 mesh copper grids using ethanol as a solvent. Micrographs were taken using a Philips 420T scanning transmission electron microscope (STEM) operating at an accelerating voltage of 100 kV.

Dynamic mechanical analysis (DMA) was carried out in the tensile mode using a Seiko model 210. The samples, which had dimensions of approximately 15 x 5 x 5 mm^3, were heated from –120 °C to 250 °C at a rate of 2.0 °C/min. The storage modulus and tanδ data were collected at a frequency of 1 Hz. The grip-to-grip distance was set at 10 mm. Storage moduli for the foams were arbitrarily normalized to 3 x 10^9 Pa in the glassy state to remove the effect of differences in cellular structure and bulk foam densities.

Differential scanning calorimetery (DSC) experiments were conducted using a Seiko DSC 220C at a heating rate of 10 °C/min and using a nitrogen purge. DSC was carried out to observe any changes in the soft segment glass transition temperature position and breadth on changing the ratios of the isocyanate isomers.

7.4 Results and Discussion

SEM images for foams T65, T80, and T100, parallel and perpendicular to the blow direction, are shown in Figure 7.2. All three foams exhibit anisotropic cellular structures, as expected, where the cells appear more elongated along the blow direction. This anisotropy in cellular structure and its importance with respect to mechanical behavior has been reported in previous studies.[13, 14, 24] It can be observed from these images that the size of the cells, cell size distribution, and strut thickness are comparable for all the three foams investigated. It is noted from Figures 7.2a and 7.2b that foam T65 possesses a fair number of open cells when viewed from the two orthogonal directions. The SEM of foam T80 reveals that although most of the cells

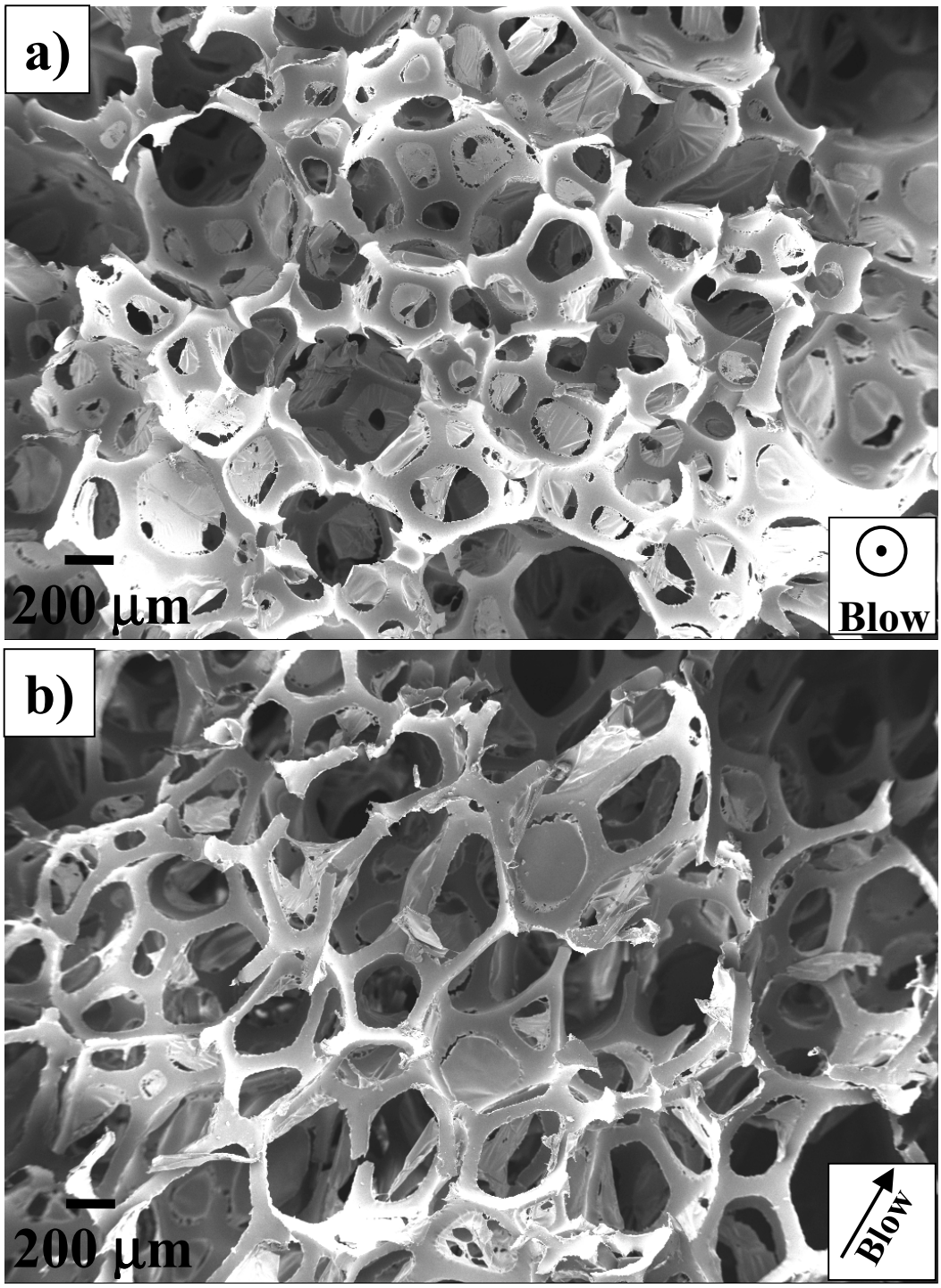

Figure 7.2 Scanning electron micrographs of the three foams a) T65 viewed parallel to blow direction b) T65 viewed perpendicular to blow direction c) T80 viewed parallel to blow direction d) T80 viewed perpendicular to blow direction e) T100 viewed parallel to blow direction f) T100 viewed perpendicular to blow direction.

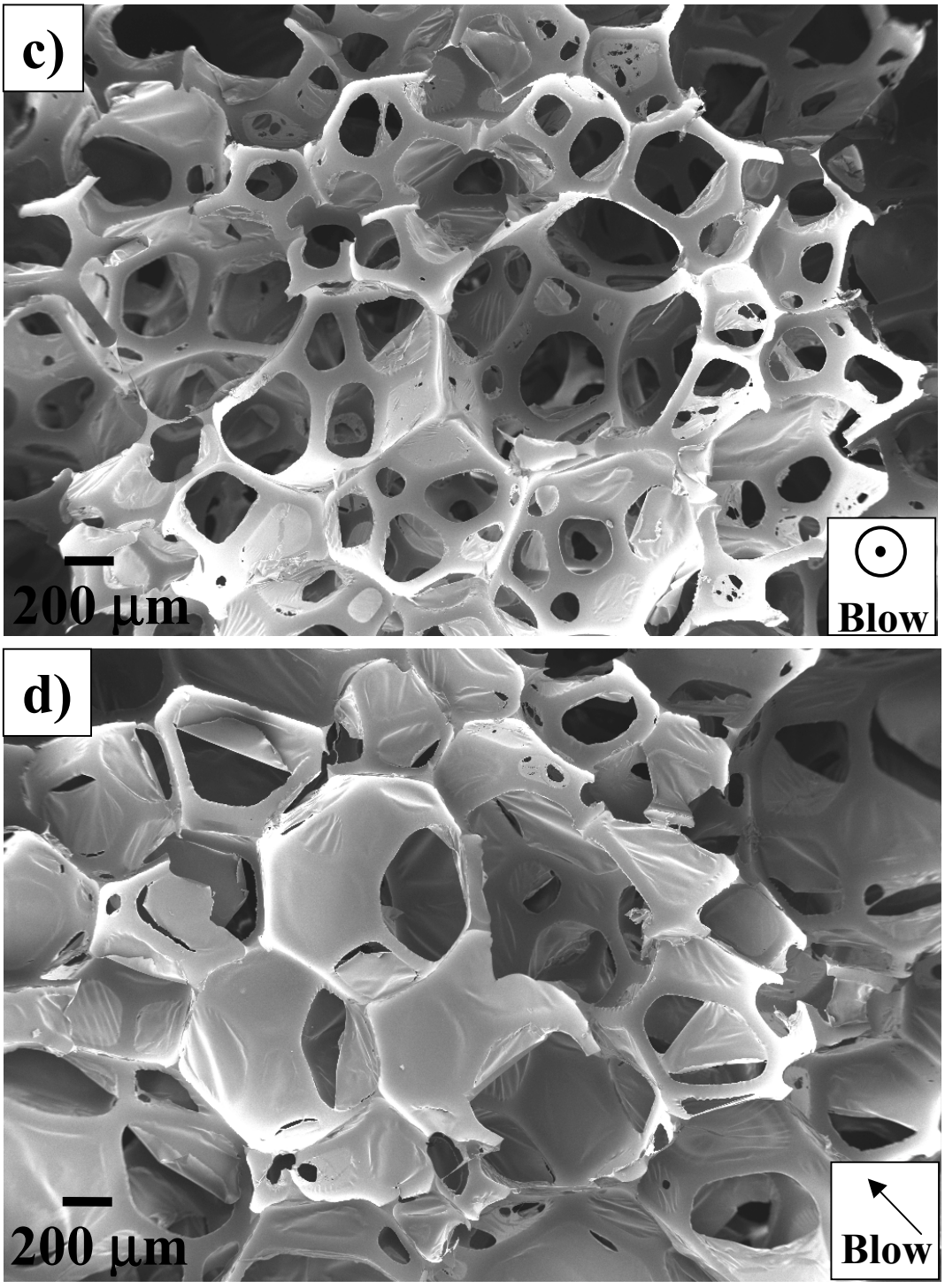

Figure 7.2 Scanning electron micrographs of the three foams c) T80 viewed parallel to blow direction d) T80 viewed perpendicular to blow direction

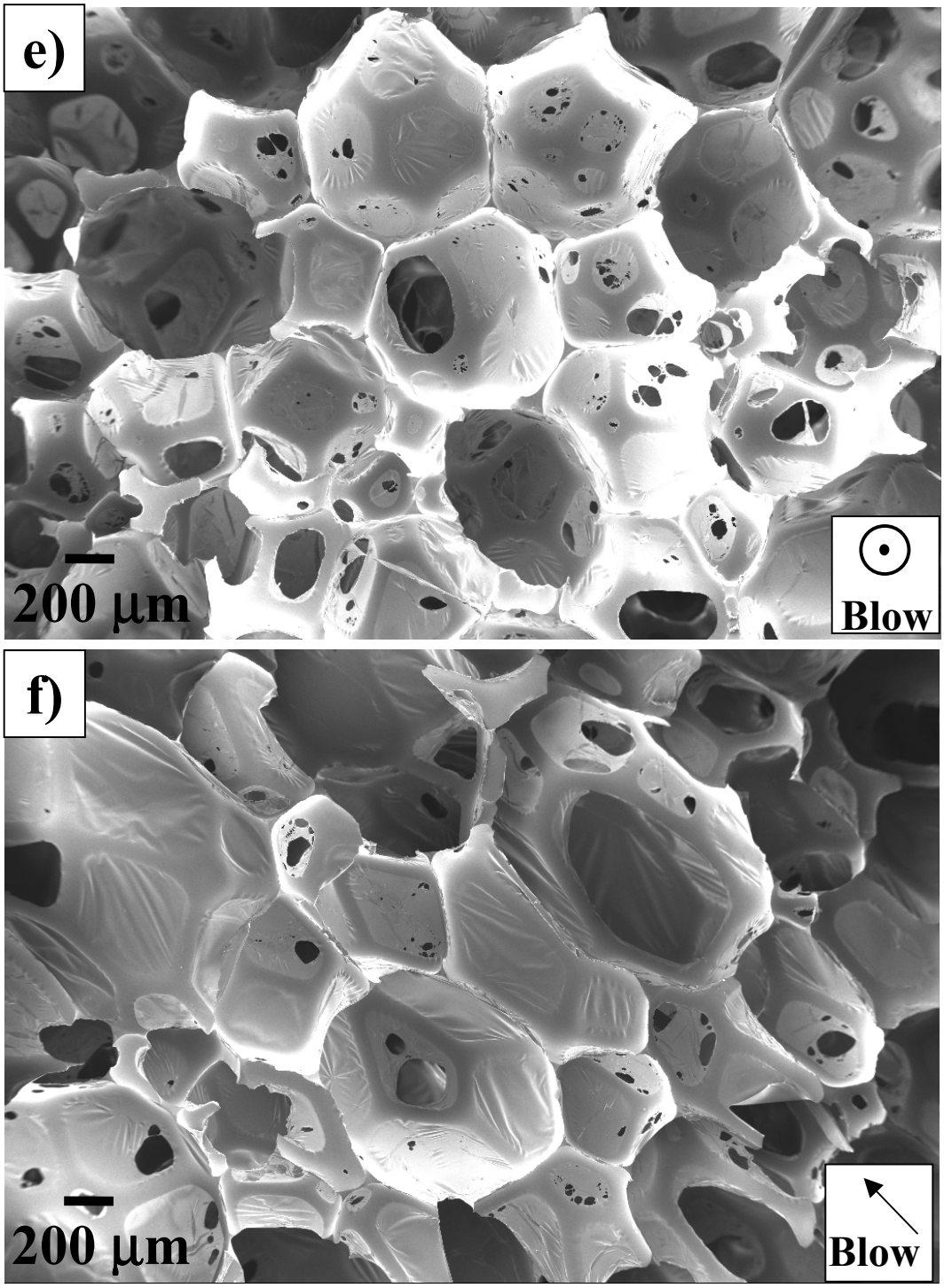

Figure 7.2 Scanning electron micrographs of the three foams e) T100 viewed parallel to blow direction f) T100 viewed perpendicular to blow direction

appear to be open when viewed parallel to the blow direction (Figure 7.2c), there are numerous cells which are still intact as seen perpendicular to the blow direction in Figure 7.2d. This difference in cell openness in the two directions is due to the differences in cell membrane characteristics (size, thickness) that are associated with the rise or blow axis relative to those orthogonal to this same axis. Finally, SEM images of foam T100 reveal that most of the cell windows of this foam are closed when viewed from both orthogonal directions. The bulk densities of the foams are presented in Table 7.1. These are noted to be in agreement with reported bulk densities of 16 – 64 kg/m^3 (1 – 4 lb/ft^3) of flexible polyurethane foams.[11] Also, the bulk foam density would be expected to be a function of the amount of intact cellular material. Accordingly, it is observed from Table 7.1 that foam T100 has a density which is slightly higher compared to the other two foams which have comparable densities.

The urea aggregation behavior of these materials was investigated using TEM, and the results from this technique are presented in Figure 7.3. The urea aggregates appear as darker regions on the micrographs due to their greater electron density as compared to the surrounding polyol phase which appears lighter. It can be seen from these images that the three foams display marked differences in the urea aggregation behavior. (Recall that all three foams are based on 5 water pphp, i.e., the hard phase content is the same and equal to 32 wt. % for all the three foams.) Foam T65 distinctly displays the largest urea aggregates, approximately 0.4 – 0.5 μm in size. This foam also displays urea aggregates which are lathe-like in appearance in contrast to foams T80 and T100 where the aggregates are more spherical in shape. It can also be observed that the size of urea aggregates is ca. 0.2 – 0.3 μm in foam T80, where as in foam T100 most of the urea aggregates are typically smaller than 0.2 μm in size. Previous studies have shown that the precipitation of the urea phase and the formation of urea aggregates are directly related to the cell-opening event in flexible polyurethane foams.[25, 26] Clearly, foam T65 displays the highest level of urea aggregation and thus results in the maximum number of open cell windows, as observed earlier by SEM. Foam T80 possessed smaller aggregates as compared to foam T65 and thus leads to it possessing an intermediate number of closed windows. Foam T100, which utilizes pure 2,4 TDI exhibits the least urea phase aggregation and the maximum amount of closed cellular material.

SAXS profiles for foams T65, T80, and T100 are shown in Figure 7.4. At lower values of the scattering vector ‘s’, (where $s = (2/\lambda)\sin(\theta/2)$, λ is the wavelength of the X-ray source, and θ

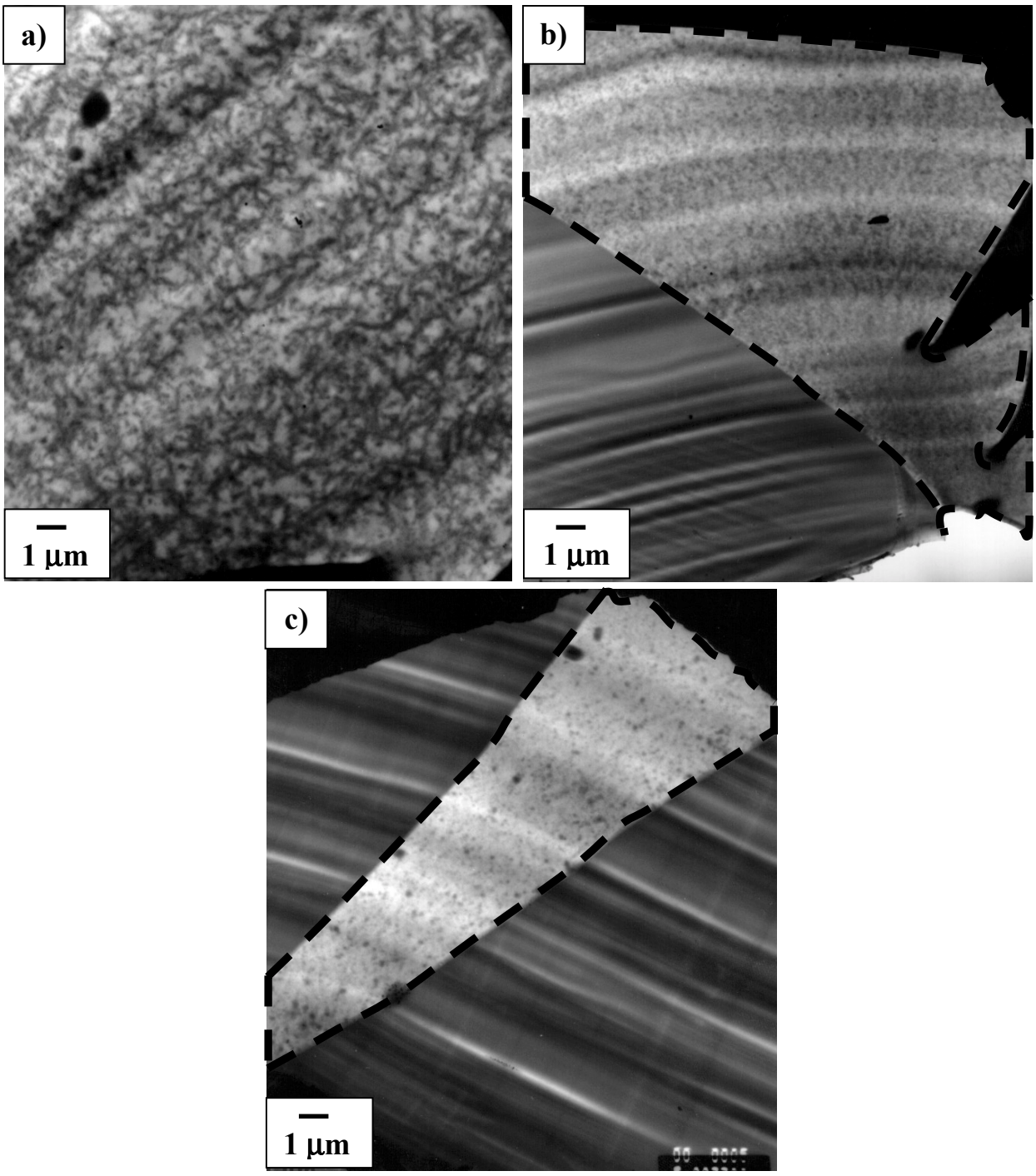

Figure 7.3 Differences in urea aggregation as observed by TEM a) T65 b) T80 c) T100. ***Note that the epoxy which was used to embed the samples is visible in the micrographs of foams T80 and T100. The foam struts are only those regions which display the urea aggregation, and are enclosed by a dashed boundary.***

the radial scattering angle), the observed upturn in the SAXS intensity is attributed to the presence of both, the presence of the large urea rich aggregates, as well as due to the cellular nature of the foam. It is also noted that all three foams display a first order interference in the form of a shoulder at an approximate 's' value of 0.01 $Å^{-1}$. This suggests that all foams display some level of microphase separation, with an interdomain spacing of ca. 100 Å, in agreement with previously reported results.[11, 13] It can also be observed on close inspection of the shoulder region that foam T65 displays the relatively 'weakest' shoulder and foam T100 the relatively 'sharpest' shoulder. This suggests that the interdomain spacing is relatively the most periodic in foam T100 where as foam T65 has relatively the widest distribution of interdomain spacings. This observation can be further explained by the fact that the aggregation of the urea phase, as observed via TEM, is observed to be the least in foam T100, thus suggesting that the urea microdomains are distributed most uniformly in this material and thus leading to the relatively sharpest SAXS shoulder. Foam T65 exhibits the highest level of urea aggregation amongst all

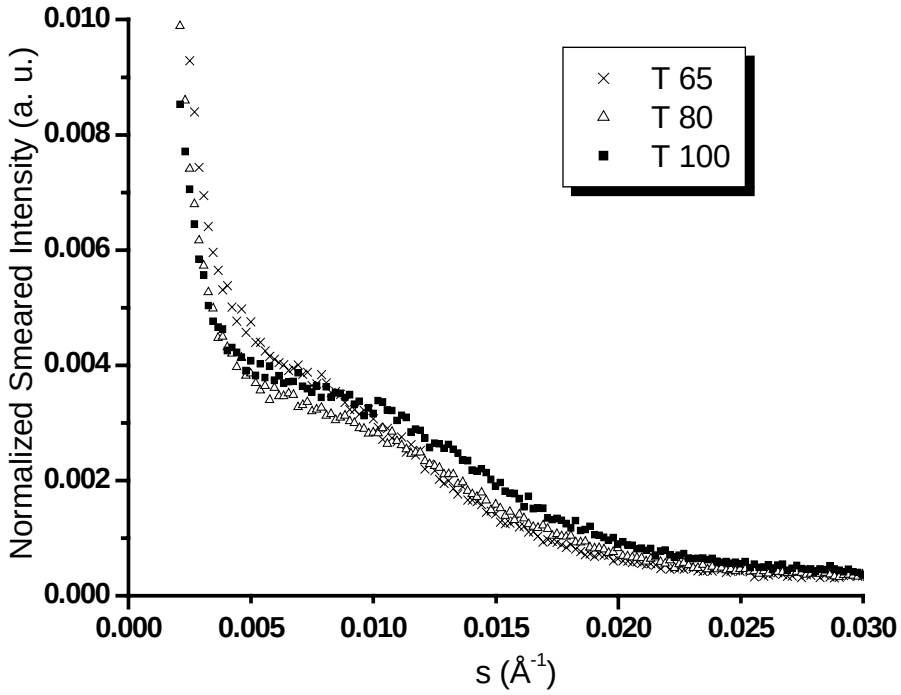

Figure 7.4 Effect of TDI isomer content on SAXS profiles for the three foams investigated.

three foams, and in this material numerous urea microdomains are present in the urea rich aggregates as well as in the surrounding polyol matrix. Hence there is a wider distribution of the interdomain spacing in this system and a weaker SAXS shoulder is observed for this foam. The above observations are also supported by a previously reported study from our laboratory where

it was noted that the incorporation of lithium chloride in plaques based on molded foam formulations suppressed the formation of urea aggregates and resulted in a corresponding sharpening of the SAXS shoulder.[10]

Hydrogen bonding is known to play an important role in determining the morphology as well as mechanical properties of a variety of polymers such as polyurethanes, poly(urethane ureas), polyamides, polyvinyl alcohol amongst other polymers which are capable of forming hydrogen bonds.[27, 28, 29] The urea microdomains in polyurethane foams are known to possess bidentate hydrogen bonding which is associated with a 1640 cm^{-1} absorbance observed via FTIR.[9] The presence of hydrogen bonding also leads to the hard segments packing in an organized manner, which is not truly crystalline, but can be detected by a 4.7 Å reflection via WAXS.[9] Normalized FTIR scans for the three foams investigated are shown in Figure 7.5. It can

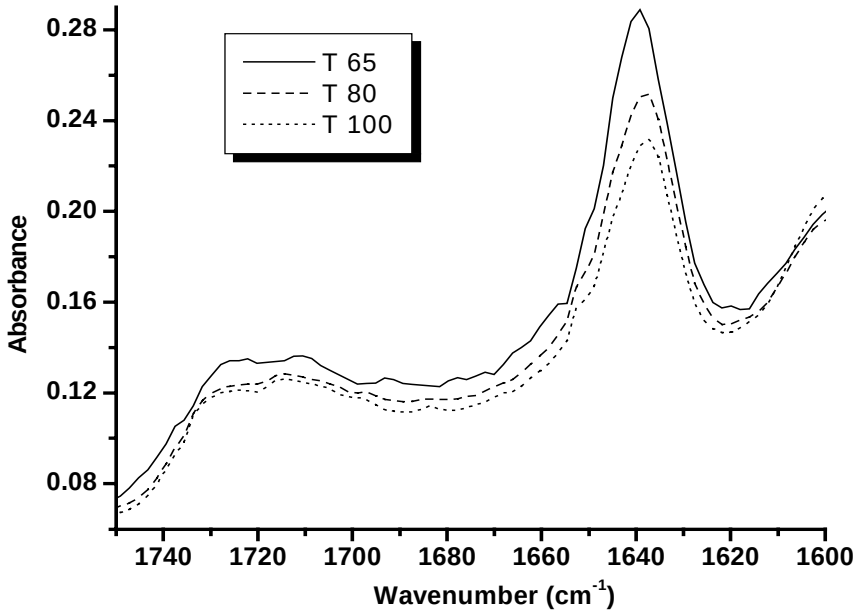

Figure 7.5 Portion of FTIR spectrum showing influence of the TDI isomer content on the hydrogen bonding characteristics of foams T65, T80, and T100.

be noted that the hard segments in all the three foams possess bidentate hydrogen bonding as observed by the presence of a 1640 cm^{-1} peak. On comparing the data for the three foams, it is seen that foam T65 exhibits the maximum absorbance at 1640 cm^{-1}, suggesting that the hard segments in this foam possess the highest level of bidentate hydrogen bonding. The 1640 cm^{-1} absorbance is found to decrease as the 2,4 TDI isomer content is increased, thus suggesting that the symmetry of the isocyanate moiety has a considerable impact on the packing behavior of the

urea hard segments within the urea microdomains. As referenced earlier, studies carried out by Sung and Schneider also suggested that polyurethane elastomers based on the 2,6 TDI isomer exhibit a higher extent of hydrogen bonding as compared to elastomers based on 2,4 TDI.[18] WAXS patterns (not shown in this chapter) for all three foams display a 4.7 Å d-spacing, suggesting that the nature of short-range ordering of the hard segments is similar in all three foams.

DSC and DMA were used to ascertain differences in the soft segment glass transition of the three foams analyzed. The soft segment T_g was determined as the inflexion point from the DSC glass transition region and as the peak Tanδ position from DMA. DSC results are presented

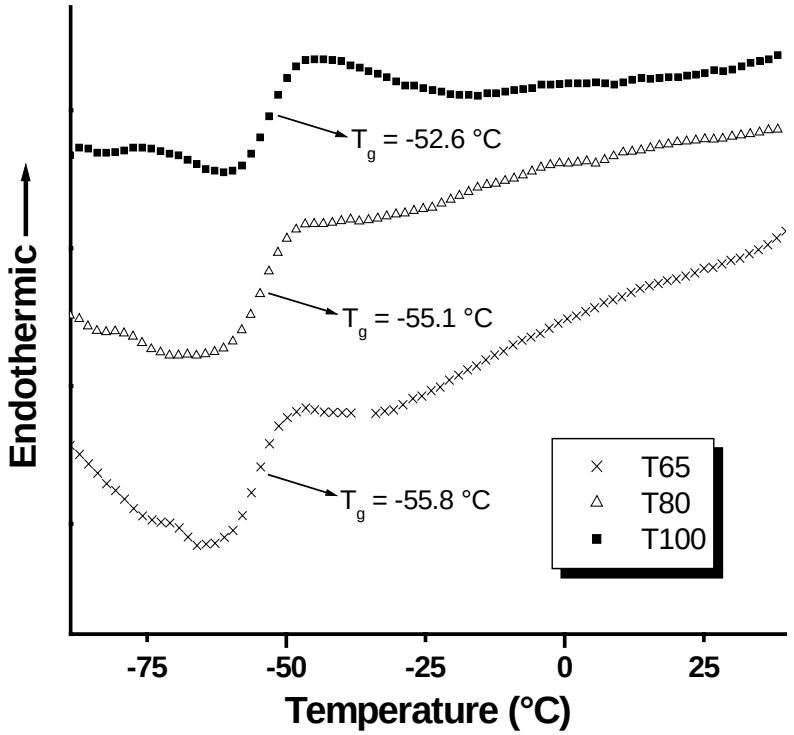

Figure 7.6 Soft segment glass transition region as observed from DSC for foams T65, T80, and T100.

in Figure 7.6, DMA results in Figure 7.7(a) and the soft segment T_g values obtained are summarized in Table 7.2. Clearly, both techniques demonstrate that the soft segment T_g decreases as the content of the symmetric 2,6 TDI isomer is increased. As discussed earlier, a similar trend was noted by Nierzwicki on examining a series of polyurethane elastomers with varied contents of the 2,4 and 2,6 TDI isomer ratios.[19] This observed trend suggests that an increase in the content of the symmetric isomer enhances the perfection of microphase-

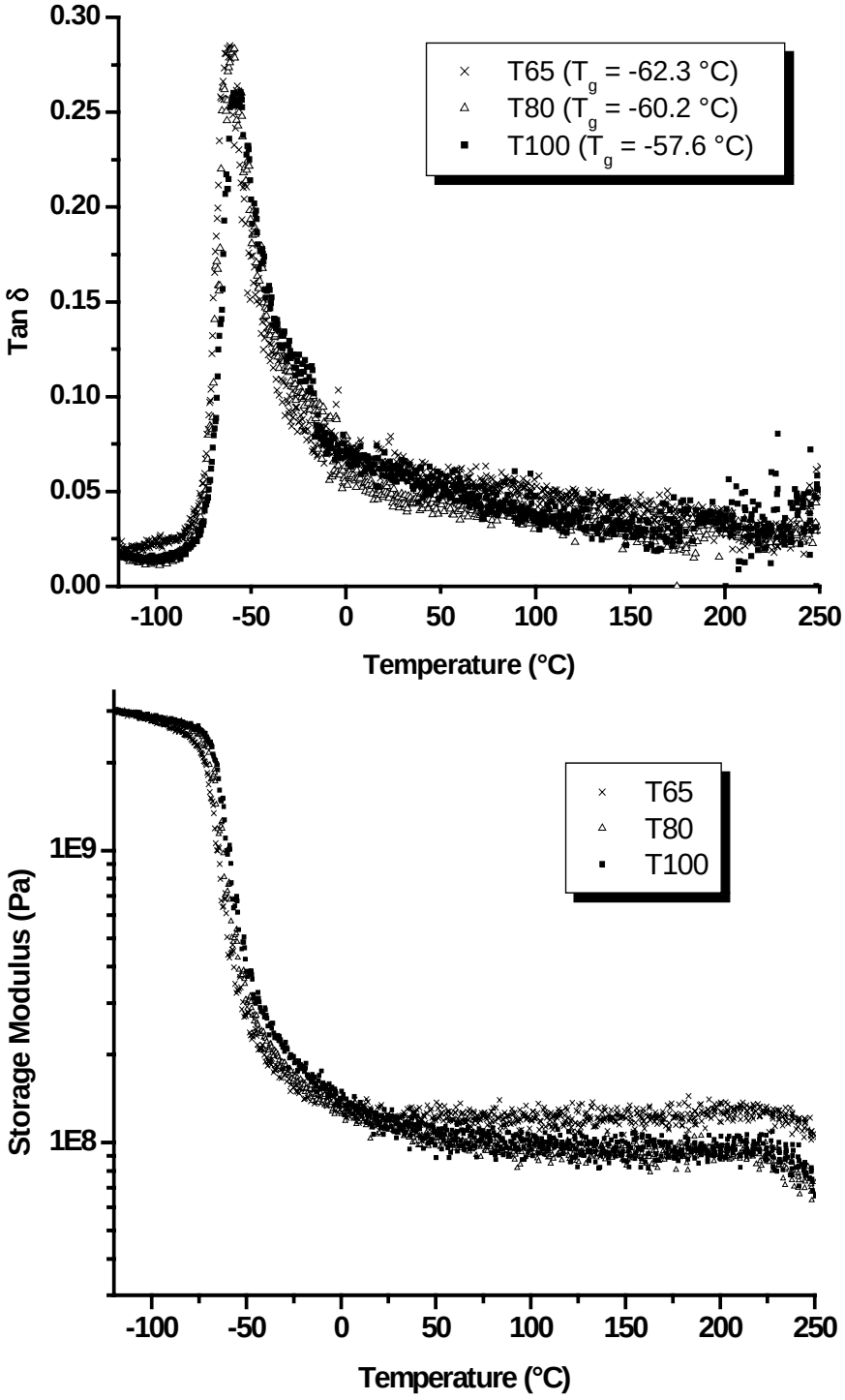

Figure 7.7 Influence of TDI isomer content on (a) Tanδ (b) Storage modulus, as determined by DMA.

separation. A lower soft segment T_g would generally imply that the urea microdomains are better separated from the polyol.

Storage moduli data as obtained from DMA for the three foams are presented in Figure 7.7(b). It can be observed that foam T65 displays the highest modulus in the rubbery region. Since the phase separated urea microdomains are a major factor in determining the physical

Sample	T_g (°C) (from inflexion point in DSC curve)	T_g (°C) (from peak Tanδ position in DMA)
T65	-55.8	-62.3
T80	-55.1	-60.2
T100	-52.6	-57.6

Table 7.2 Soft Segment T_g values as obtained from DSC and DMA

properties of these materials, it is thought that the polymer would become stiffer when the concentration of the symmetric 2,6 TDI isomer used in the formulation is increased. Due to the symmetrical nature of the 2,6 TDI isomer, it is expected that as the content of this isomer is increased, the hard segments formed would be more linear in nature which would in turn improve their local packing characteristics. The presence of linear hard segments would also help promote the formation of urea microdomains which have higher aspect ratios as compared to when the content of the 2,6 TDI isomer is lower, in which case more spherical microdomains might be expected to form. The formation of high aspect ratio microdomains would enhance the interconnectivity of the urea phase, and hence the stiffness of the foam. Increasing the 2,6 TDI isomer content also increases the perfection of microphase separation as noted by a decrease in the soft segment T_g, and also enhances the formation of the urea aggregates, as was observed by TEM. These factors, along with the observed increase in bidentate hydrogen-bonding on increasing the 2,6 isomer content are believed to explain why foam T65 exhibits the highest rubbery modulus.

7.5 Conclusions

The morphology as well as the dynamic mechanical behavior of three foams based on 65:35 2,4/2,6 TDI, 80:20 2,4/2,6 TDI, and 100:0 2,4/2,6 TDI have been investigated. SEM was used to note differences in the cellular structure of the three foams. The foams were noted to possess varying degrees of cell-openness for which a possible explanation was given by noting

differences in the urea aggregation behavior of the foams via TEM. SAXS results indicated that all three foams were microphase separated and possessed similar interdomain spacings. DSC and DMA showed that the soft segment T_g decreased as the content of the 2,6 TDI isomer was increased – thus suggesting that the perfection of microphase separation was enhanced on increasing the symmetric isomer content. FTIR revealed that an increase in the content of the symmetric 2,6 TDI isomer increased the level of hydrogen bonding of the hard segments. The increased level of phase separation and hydrogen bonding in the foam containing the 65:35 TDI isomer mixture led to its possessing the highest rubbery modulus as noted by DMA.

The issue of 'connectivity' or the continuity of the hard phase has been of interest to workers in the area of polyurethanes. Hydrogen bonding of the hard segments results in these materials possessing inter-segmental connectivity. In the case of polyurethane foams, aggregation of the urea phase at the micron level leading to an increase in connectivity at the urea aggregate level may play an important role in determining the mechanical properties of the foam. Greater inter-segmental connectivity as observed by FTIR, and also greater urea aggregate connectivity as observed via TEM is thought to play an important role in enhancing the rubbery modulus of foam T65. The issue of urea phase connectivity at different length scales has been indirectly addressed in the same laboratory using the cross-linking agent diethanol amine (DEOA)[30] and is currently being probed more directly using LiCl as an additive.[10, 31]

7.6 References

1. Hepburn, C. In Polyurethane Elastomers, 2nd ed.; Elsevier Applied Science: London, 1991.
2. Neumüller, W.; Bonart, R. J Macromol Sci Phys 1982, B(21)2, 203-217.
3. Tyagi, D.; McGrath, J.E.; Wilkes, G.L. Polym Eng Sci 1986, 26, 1371-1398.
4. Koberstein, J.T.; Stein, R.S. J Polym Sci Polym Phys 1983, 21, 1439-1472.
5. Abouzahr, S.; Wilkes, G.L.; Ophir Z. Polymer 1982, 23, 1077-1086.
6. Christenson, C.P.; Harthcock, M.A.; Meadows, M.D.; Spell, H.L.; Howard, W.L.; Creswick, M.W.; Guerra, R.E.; Turner, R.B. J Polym Sci Polym Phys 1986, 24, 1401-1439.
7. McLean, R.S.; Sauer, B.B. Macromolecules 1997, 30, 8314-8317.
8. Garrett, J.T.; Runt, J.; Lin, J.S. Macromolecules 2000, 33, 6353-6359.
9. Kaushiva, B.D.; McCartney, S.R.; Rossmy, G.R.; Wilkes, G.L. Polymer 2000, 41, 285-310.
10. Aneja, A.; Wilkes, G.L. J Appl Polym Sci 2002, 85, 2956-2967.

11. Herrington, R.; Hock, K. In Flexible polyurethane foams, 2nd ed.; Dow Chemical Co.: Midland, MI, 1998.
12. Ade, H.; Smith, A.P.; Cameron, S.; Cieslinski, R.; Mitchell, G.; Hsiao, B.; Rightor, E. Polymer 1995, 36, 1843-1848.
13. Armistead, J.P.; Wilkes, G.L.; Turner, R.B. J Appl Polym Sci 1988, 35, 601-629.
14. Moreland, J.C.; Wilkes, G.L.; Turner, R.B. J Appl Polym Sci 1994, 52, 549-568.
15. Moreland, J.C.; Wilkes, G.L.; Turner, R.B. J Appl Polym Sci 1994, 52, 569-576.
16. Gmitter, G.T.; Gruber, E.E. SPE Journal 1957, 13/1, 27-30.
17. Smith, C.H.; Petersen, C.A. SPE Journal 1962, 18/4, 455-459.
18. Sung, C.S.P.; Schneider N.S. Macromolecules 1975, 8, 68-73.
19. Nierzwicki, W. J Appl Polym Sci 1990, 41, 907-915.
20. Molau, G.E. In Colloidal and Morphological Behavior of Block and Graft Copolymers; Plenum Press: New York, 1971.
21. Matsen M.W.; Schick, M. Phys Rev Lett 1994, 72, 2660-2663.
22. Bates, F.S.; Fredrickson, G.H. Phys Today 1999, 52/2, 32-38.
23. Seymour, R.W.; Cooper, S.L. Adv Urethane Sci 1974, 3, 66-80.
24. Moreland, J.C.; Wilkes, G.L.; Turner, R.B.; Rightor, E.G. J Appl Polym Sci 1994, 52, 1459-1476.
25. Rossmy, G.L.W.; Schator, H.; Wiemann, M.; Kollmeier, H.J. J Cell Plast 1981, 17, 319-327.
26. Neff, R.A.; Macosko, C.W. Rheologica Acta 1996, 35, 656-666.
27. Abouzahr, S.; Wilkes, G.L. J Appl Polym Sci 1984, 29, 2695-2711.
28. Yilgör, E.; Burgaz, E.; Yurtsever, E.; Yilgör, İ. Polymer 2000, 41, 849-857.
29. Marten, F.L. Vinyl Alcohol Polymers. Encycl Polym Sci Tech, Wiley, New York, 1985, 17, 167-198.
30. Kaushiva, B.D.; Wilkes, G.L. J Appl Polym Sci 2000, 77, 202-216.
31. Aneja, A.; Wilkes, G.L. Polymer 2002, 43, 5551-5561.